

ARTICLE OPEN



Pathogenic gene connections in type 2 diabetes and non-alcoholic fatty liver disease: a bioinformatics analysis and mouse model investigations experiments

Chao Chen^{1✉}, Kunhuan Yang¹, Yuhan Zhang¹, Meiqi Lu², Xiaoyan Zhao² and Zheng Wan^{2✉}

© The Author(s) 2024

BACKGROUND: Type 2 diabetes (T2D) and non-alcoholic fatty liver disease (NAFLD) are prevalent metabolic disorders with overlapping pathophysiological mechanisms. A comprehensive understanding of the shared molecular pathways involved in these conditions can advance the development of effective therapeutic interventions.

METHODS: We used two datasets sourced from the Gene Expression Omnibus (GEO) database to identify common differentially expressed genes (DEGs) between T2D and NAFLD. Subsequently, we conducted Gene Ontology (GO) and Kyoto Encyclopedia of Genes and Genomes (KEGG) analyses to identify the enriched biological processes and signaling pathways. In addition, we performed a protein-protein interaction (PPI) network analysis to identify hub genes with pivotal roles. To validate our findings, we established a type 2 diabetic mouse model with NAFLD.

RESULTS: Our analysis identified 53 DEGs shared between T2D and NAFLD. Enrichment analysis revealed their involvement in signal transduction, transcriptional regulation, and cell proliferation as well as in the ferroptosis signaling pathways. PPI network analysis identified ten hub genes, namely *CD44*, *CASP3*, *FYN*, *KLF4*, *HNRNPM*, *HNRNPU*, *FUBP1*, *RUNX1*, *NOTCH3*, and *ANXA2*. We validated the differential expression of *FYN*, *HNRNPU*, and *FUBP1* in liver tissues of a type 2 diabetic mouse model with NAFLD.

CONCLUSIONS: Our study offers valuable insights into the shared molecular mechanisms underlying T2D and NAFLD. The identified hub genes and pathways present promising prospects as therapeutic targets to address these prevalent metabolic disorders.

Nutrition and Diabetes (2024)14:60; <https://doi.org/10.1038/s41387-024-00323-0>

INTRODUCTION

Diabetes is a chronic condition characterized by insufficient insulin (type 1 diabetes) or impaired insulin function (type 2 diabetes), resulting in elevated blood glucose levels [1]. Type 2 diabetes (T2D) is the most prevalent type of diabetes, and poses a significant threat to human health. The incidence of diabetes is high, with approximately 463 million individuals worldwide estimated to have diabetes as of 2019, according to the World Health Organization (WHO) [2]. Recently, diabetes has become more common worldwide, mainly because more people are becoming inactive. T2D can lead to various complications, including cardiovascular diseases, neuropathy, diabetic nephropathy and non-alcoholic fatty liver disease (NAFLD), and has garnered significant attention worldwide [3, 4].

NAFLD is a chronic metabolic disorder characterized by excessive hepatic fat accumulation, unrelated to alcohol consumption. It has a global prevalence of 25.2% [5]. The exact cause of NAFLD is not fully understood, but it is believed to be strongly associated with T2D [6]. A study has revealed that over 22.51% of individuals diagnosed with T2D also exhibit NAFLD [5]. Furthermore, the relationship between T2D and NAFLD is bidirectional [7]. Individuals with T2D often present with metabolic dysfunction,

which collectively contributes to the pathogenesis of NAFLD [8]. In addition, NAFLD can adversely affect individuals with T2D, increasing their susceptibility to complications [9]. However, the association between NAFLD and T2D is not yet fully understood, indicating the need for further research to understand this association better.

Liver enzyme and function tests, imaging examinations, and liver biopsies are commonly used diagnostic methods for NAFLD [10]. However, each of these approaches has inherent limitations. For instance, liver enzyme and function tests cannot directly diagnose NAFLD [6]. Similarly, imaging methods fail to provide intricate pathological information and may exhibit reduced sensitivity for detecting mild cases of NAFLD [11]. Moreover, a liver biopsy is invasive and can be subject to sampling errors [12, 13]. Therefore, further studies are needed to develop innovative diagnostic methods.

This study used bioinformatics and systems biology techniques to examine how certain molecular processes could help treat T2D and NAFLD. GSE185011 and GSE89632 were retrieved from the Gene Expression Omnibus (GEO) database to determine the biological relationships between T2D and NAFLD. Next, common differentially expressed genes (DEGs) shared between these two

¹Institute of Genomics, School of Medicine, Huaqiao University, 668 Jimei Road, Xiamen 361021, China. ²School of Medicine, Xiamen University, Xiamen 361000, China.

✉email: chenchaoh@hqu.edu.cn; wanzheng0626@xmu.edu.cn

Received: 6 December 2023 Revised: 20 July 2024 Accepted: 25 July 2024

Published online: 06 August 2024

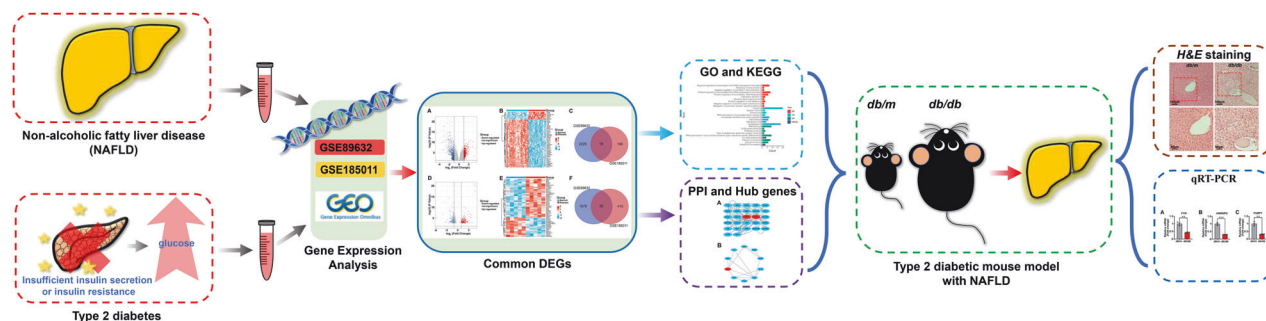


Fig. 1 Schematic diagram of the overall workflow of this study. The study retrieved datasets GSE185011 and GSE89632 from the GEO database to explore the relationship between type 2 diabetes (T2D) and non-alcoholic fatty liver disease (NAFLD). Common differentially expressed genes (DEGs) were identified using GEO2R. Gene Ontology (GO) and KEGG enrichment analyses were performed on these DEGs. A protein–protein interaction (PPI) network identified hub genes. Validation was done using a type 2 diabetic mouse model with NAFLD (*db/db* mice), identifying three key genes.

Table 1. A Summary of GEO-derived Datasets.

Series	Platforms	Chip Gene	Disease	Normal
GSE185011	GPL24676	Illumina NovaSeq 6000	5	5
GSE89632	GPL14951	Illumina HumanHT-12 WG-DASL V4.0 R2 expression bead chip	19	24

diseases were identified using GEO2R. Gene Ontology (GO) and Kyoto Encyclopedia of Genes and Genomes (KEGG) enrichment of mutual DEGs was performed using bioinformatics tools. The protein-protein interaction network (PPI) was used to search for hub genes. Finally, a type 2 diabetic mouse model with NAFLD (genetically diabetic leptin receptor-mutated (*db/db*) mice) was used to validate the prediction results, and three genes were identified. The sequential workflow of this study is illustrated in Fig. 1.

MATERIALS AND METHODS

Data extraction

We obtained data from the GEO (<https://www.ncbi.nlm.nih.gov/geo/>) [14] to identify the common genetic linked between T2D and NAFLD. The diabetic dataset GSE185011 (GPL24676 platform) included peripheral blood samples from 5 healthy individuals and 5 patients with T2D. The NAFLD dataset GSE89632 (GPL14951 platform) included 24 healthy individuals and 19 patients with NAFLD (Table 1).

Identification of DEGs

The DEGs in peripheral blood samples from patients and the control group were analyzed using GEO2R [14] software with adjusted $P < 0.05$, $\log_2FC > 1$ as up regulation, and $\log_2FC < -1$ for DEGs as down regulation. This study used Venn software to check for crossover DEGs.

GO and KEGG pathway enrichment

GO and KEGG analysis was performed using the DAVID database [15] (<https://david.ncifcrf.gov/>) to investigate possible functions, including biological process (BP), molecular function (MF), and cellular component (CC) as well as pathways enriched in these DEGs. Statistical significance was set at adjusted $P < 0.05$.

PPI network construction and hub gene extraction

The STRING database (<https://www.STRING-db.org>) [16] was used to build PPI networks to examine the relationships between two datasets. Cytoscape software (v3.9.0) (<https://www.cytoscape.org/>) was used to visualize and analyze the PPI network. Additionally, the CytoHubba plugin [17] in Cytoscape was used to select the ten hub genes.

Animals

The Institutional Animal Care and Use Committee of the Huaqiao University School of Medicine approved this animal study. The lean leptin

gene knockout mice (*db/db*) and non-homozygous littermates (*db/m*) were a gift from professor Qian Chen (Xiamen University, China). After rearing neonatal *db/db* and *db/m* mice under standard feeding conditions until 8 months of age, the mice were photographed and analyzed. Their body and liver weights were recorded, blood glucose levels were measured, and complete liver specimens were excised and photographed for subsequent analyses. Male *db/db* and *db/m* mice with C57BL/6 J genetic background were used in this study. The mice were randomly divided into two groups (*db/db* and *db/m*) with at least three mice in each group.

Hematoxylin and eosin staining

The mouse liver was fixed at 4 °C polyformaldehyde for 2 days, followed by embedding in paraffin. Paraffin-embedded tissues were sectioned at 5 μm thickness, and subsequently stained with hematoxylin and eosin (H&E) staining. Images were captured using a Leica camera.

Quantitative real-time polymerase chain reaction (qRT-PCR)

Total RNA was isolated from the liver using TRNzol Universal Reagent. For cDNA synthesis, 2 μg of the isolated total RNA was used as the template. RNA was reverse transcribed to cDNA using the ReverTra Ace qPCR RT Master Mix kit (Toyobo, Osaka, Japan). qRT-PCR analysis was conducted using a Stratagene™ Mx3005P qPCR Instrument to determine the expression levels of the target genes. The data acquired for each target gene were normalized using GAPDH as an internal reference gene. All primers were designed using the NCBI for Biotechnology Information Primer Design Tool. Primers were synthesized by Sangon Biotech Company (Shanghai, China), and their details are presented in Table 2.

Statistics analysis

A moderated t -test was used to identify the DEGs, and statistical significance was set at an adjusted $P < 0.05$ using the Benjamini & Hochberg method [18]. The qRT-PCR data were analyzed using the GraphPad Prism software (version 8.0; La Jolla, CA, USA). All qRT-PCR data are expressed as the mean \pm standard deviation (SD) from a minimum of three independent experiments. Statistical analyses for animal experiments were conducted using the Student's t -test and statistical significance was set at $P < 0.05$.

RESULTS

Common DEGs identification

First, 3856 DEGs were discovered in GSE89632; out of these, 2243 were upregulated and 1613 were downregulated. In GSE185011, 656 DEGs were identified; 206 were upregulated and 450 were

Table 2. Primer sequences for qRT-PCR.

Gene	Species	Forward primer (5' → 3')	Reverse primer (5' → 3')
<i>FYN</i>	mouse	CTCAGCACTACCCAGCTTC	TCCCAGTGTGAGAGGAGGAG
<i>HNRNPU</i>	mouse	TAGAGGCCGTGGAGGATTCA	GGCCACGTGGGTATGGATAG
<i>FUBP1</i>	mouse	GCCGGATTATAGTGCAGCCT	TTATTGGCCCTGAGGTGCTG
<i>GAPDH</i>	mouse	AGGTCGGTGTGAACGGATTG	TGTAGACCATGTAGTTGAGGTCA

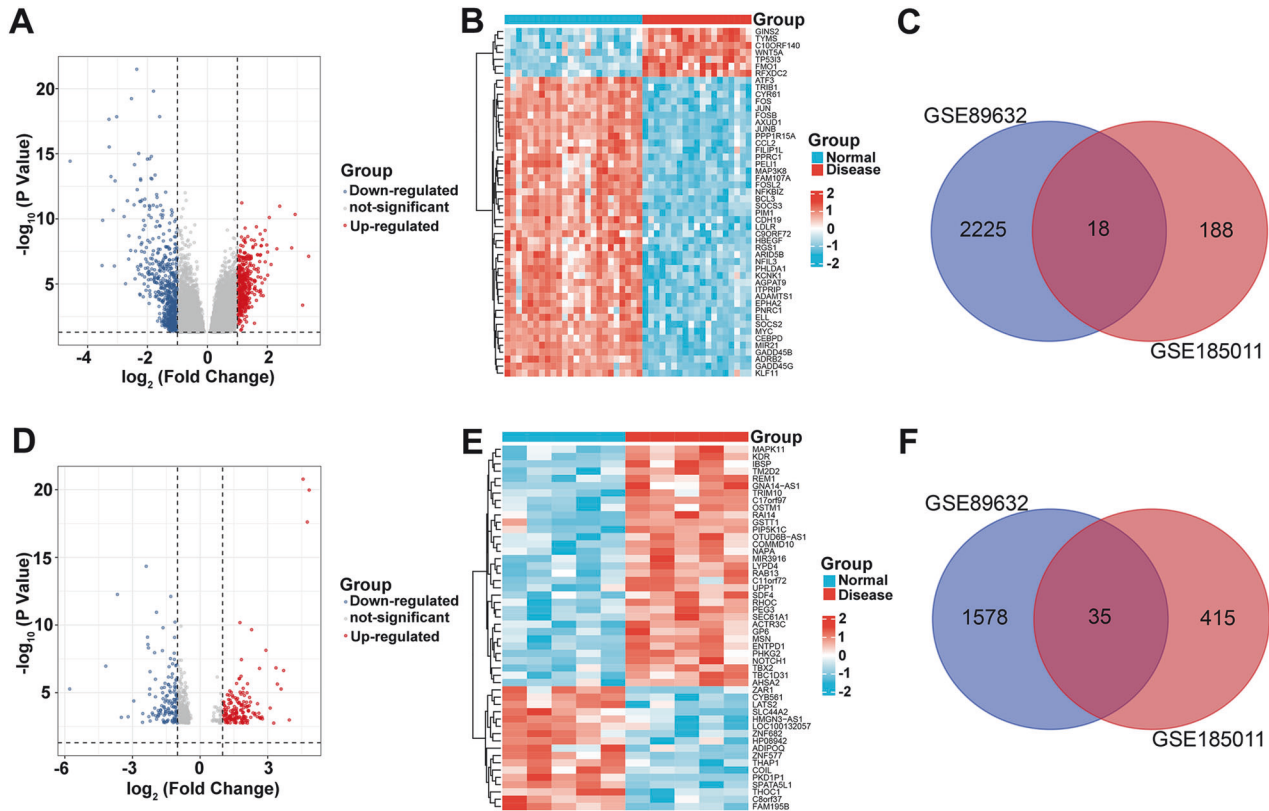


Fig. 2 Identification of differentially expressed genes (DEGs) in Type 2 diabetes (T2D) (GSE185011) and non-alcoholic fatty liver disease (NAFLD) (GSE89632) using GEO2R. **A** Volcano plots of the DEGs in GSE89632. The negative \log_{10} -transformed adjusted P values (Y axis) are plotted against the average \log_2 fold changes (X axis) in gene expressions. Identified DEGs are shown in red ($\log_2FC > 1$) and blue ($\log_2FC < -1$) with adjusted $P < 0.05$. **B** Heatmap of the DEGs in GSE89632. **C** Upregulated genes shared between GSE89632 and GSE185011. **D** Volcano plots of the DEGs in GSE185011. The negative \log_{10} -transformed adjusted P values (Y axis) are plotted against the average \log_2 fold changes (X axis) in gene expressions. Identified DEGs are shown in red ($\log_2FC > 1$) and blue ($\log_2FC < -1$) with adjusted $P < 0.05$. **E** Heatmap of the DEGs in GSE185011. **F** Downregulated genes shared between GSE89632 and GSE185011.

Table 3. Differentially expressed genes (DEGs) identification.

Terms	Gene names
Up-regulated genes	<i>CENPQ</i> , <i>ANKRD49</i> , <i>GPR174</i> , <i>SLC23A3</i> , <i>SP4</i> , <i>ZNF132</i> , <i>HBB</i> , <i>CD200R1</i> , <i>PUSL1</i> , <i>RAB26</i> , <i>KLRC2</i> , <i>ZBTB6</i> , <i>CCDC93</i> , <i>CASP3</i> , <i>ZBTB37</i> , <i>ZNF14</i> , <i>SAMD9</i> , <i>ZNF845</i>
Down-regulated genes	<i>CD44</i> , <i>NID1</i> , <i>NETO2</i> , <i>PRR16</i> , <i>STEAP3</i> , <i>RUNX1</i> , <i>FUBP1</i> , <i>KLF4</i> , <i>MYOF</i> , <i>NEDD4L</i> , <i>FYN</i> , <i>IERSL</i> , <i>HK1</i> , <i>AATF</i> , <i>UBE2L3</i> , <i>PRNP</i> , <i>ANXA2</i> , <i>CCDC149</i> , <i>GSR</i> , <i>HMOX1</i> , <i>SERPINB8</i> , <i>PTGER2</i> , <i>TLN2</i> , <i>HNRNPM</i> , <i>HNRNPAB</i> , <i>SRGAP1</i> , <i>VCAN</i> , <i>ZFH3</i> , <i>EIF3CL</i> , <i>S100A12</i> , <i>MMP19</i> , <i>NOTCH3</i> , <i>ATP2A2</i> , <i>NRG1</i> , <i>HNRNPU</i>

downregulated. We identified 53 common DEGs (18 upregulated and 35 downregulated) between the T2D and NAFLD datasets. Figure 2 shows a cross-analysis comparison of the two datasets, and Table 3 lists all DEGs.

GO and KEGG analysis

Figure 3 shows that DEGs were strongly linked to transcriptional regulation, namely regulation of transcription in the BP category;

cytosol, nuclear matrix, and endosome in the CC category; and RNA binding and ion channel binding in the MF category. Based on the KEGG pathway analysis, the most affected pathways were the ferroptosis signaling pathways.

PPI establishment and hub gene identification

Figure 4A shows the shared DEG-based PPI network with 27 nodes and 72 edges. The top ten DEGs identified were *CD44*, *CASP3*, *FYN*,

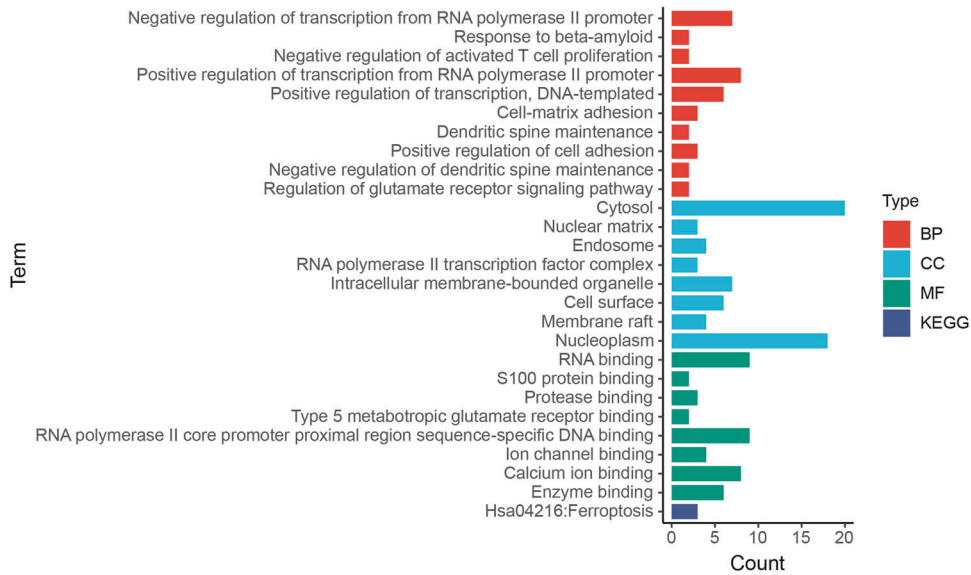


Fig. 3 Functional analyses of common differentially expressed genes (DEGs). Red, blue, green, and dark blue indicated biological process (BP), molecular function (MF), and cellular component (CC), and KEGG pathway analyses, respectively.

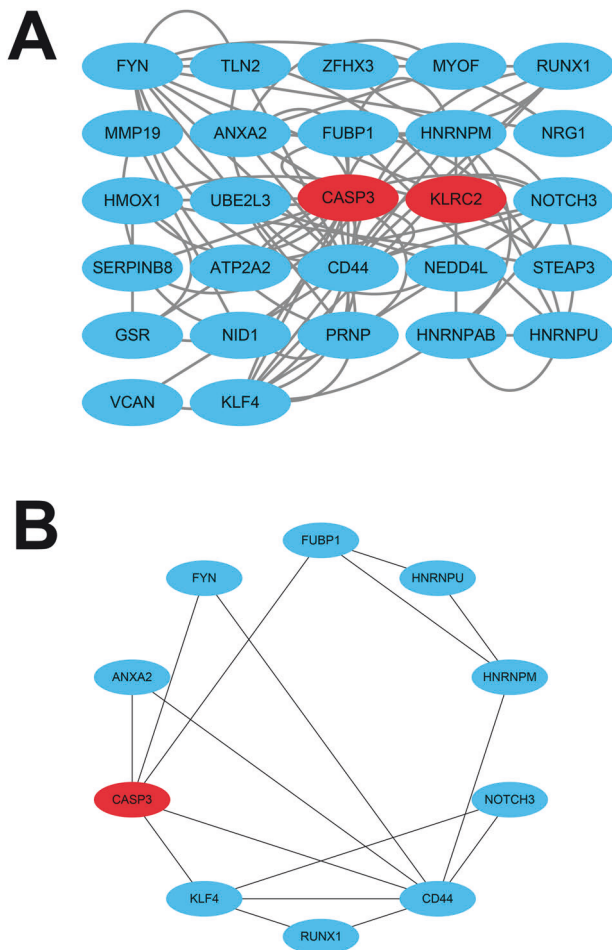


Fig. 4 Protein-protein interaction (PPI) network establishment and hub gene identification. **A** PPI network of common genes. Genes in red and blue boxes represent upregulated genes and downregulated genes, respectively. **B** Ten most significant genes involved in the PPI network.

KLRF4, *HNRNPM*, *HNRNPU*, *FUBP1*, *RUNX1*, *NOTCH3*, and *ANXA2* (Fig. 4B).

NAFLD in type 2 diabetic mouse model

To verify the gene expression in the context of T2D accompanied by NAFLD, we used *db/db* mice as an experimental model; *db/db* mice, which are characterized by leptin deficiency, serve as a robust type 2 diabetic mouse model with a profound fatty liver phenotype (Fig. 5A). In the 8-month model of *db/db* mice, we observed a significant increase in both body size and weight compared to the control group of *db/m* mice (Fig. 5B, C). Blood glucose measurements demonstrated a pronounced elevation in *db/db* mice (Fig. 5D). Furthermore, the liver images displayed notable hepatomegaly, characterized by a pale appearance and extensive lipid accumulation. Quantitative evaluation of the liver weight confirmed a substantial increase (Fig. 5E, F). Histological analysis of H&E-stained liver sections revealed prominent hepatic steatosis and disruption of normal liver tissue architecture in *db/db* mice (Fig. 5G). Taken together, these results substantiate the successful establishment of a mouse model of T2D accompanied by NAFLD.

The expression of the targeted gene was validated through qRT-PCR analysis in a type 2 diabetic mouse model with NAFLD

The qRT-PCR results showed that the mRNA expression of *FYN*, *HNRNPU*, and *FUBP1* in the livers of *db/db* and *db/m* mice was similar to that of the hub genes in the PPI analysis, and the expression levels of *FYN*, *HNRNPU*, and *FUBP1* were significantly downregulated in *db/db* mice (Fig. 6). These findings suggest that the expression of differentially expressed genes identified through bioinformatics analysis aligns with the expected trend in a type 2 diabetic mouse model with NAFLD.

DISCUSSION

Diabetes and NAFLD are two chronic metabolic disorders that have become significant threats to human health [3, 4, 19]. The prevalence of diabetes is increasingly global due to rising obesity rates and sedentary lifestyles, while NAFLD develops when fat accumulates within the liver [20]. Unraveling the molecular

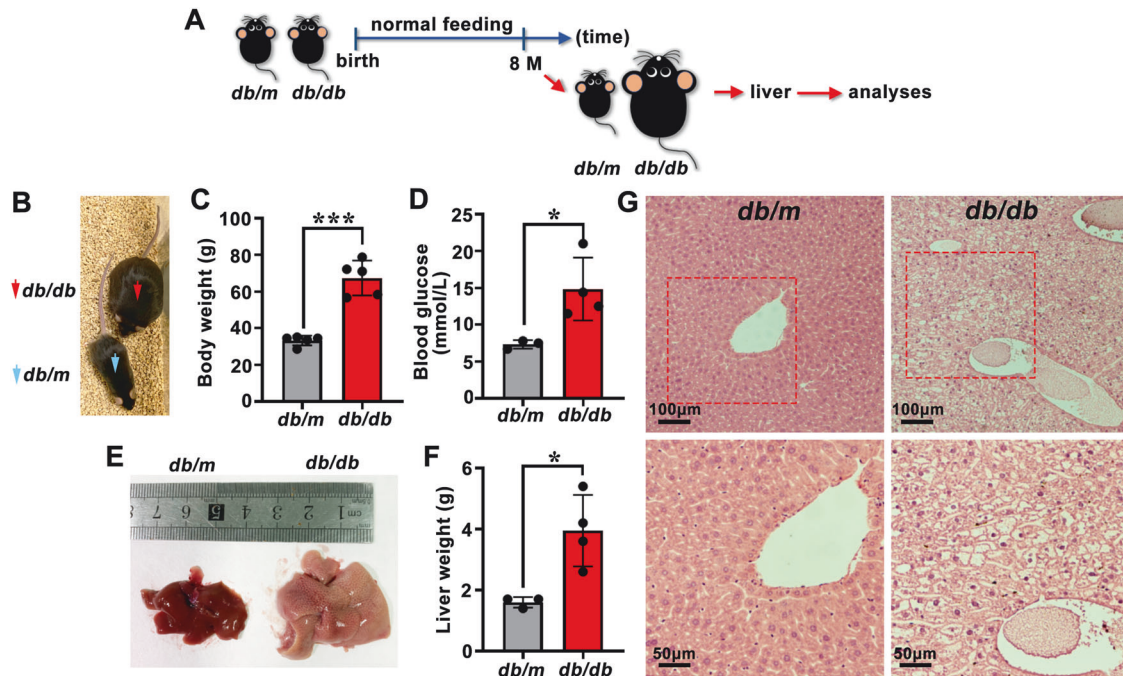


Fig. 5 Non-alcoholic fatty liver disease (NAFLD) in diabetic *db/db* mice. **A** Schematic illustration of the experimental procedure. *db/m* and *db/db* mice were fed normal diet until the age of 8 months (M). **B** Images comparing *db/m* and *db/db* mice. Blue arrows indicate *db/m* mice, red arrows indicate *db/db* mice. **C** Body weight of *db/m* and *db/db* mice. **D** Blood glucose analysis of *db/m* and *db/db* mice. **E** Images comparing the livers of *db/m* and *db/db* mice. **F** Liver weight of *db/m* and *db/db* mice. Statistical analyses in **C**, **D**, and **F** were performed using Student's *t*-test. * $P < 0.05$; *** $P < 0.001$. **G** H&E staining of liver sections from *db/m* and *db/db* mice. Scale bars, 100 μm (upper panels) and 50 μm (lower panels). Each dot represents one mouse; $n \geq 3$ in each group.

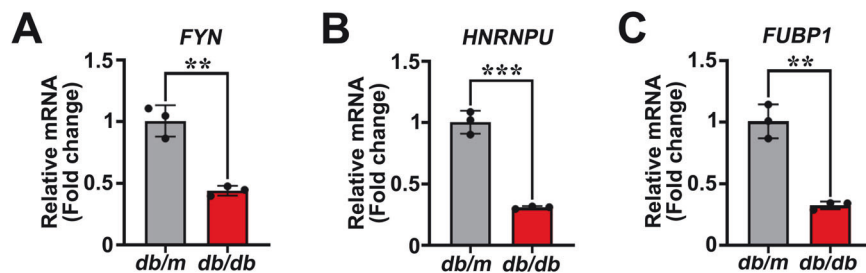


Fig. 6 The mRNA levels of *FYN*, *HNRNPU*, and *FUBP1* in *db/db* and *db/m* mouse livers. **A–C** qRT-PCR analysis of *FYN*, *HNRNPU*, and *FUBP1* in the liver of *db/db* ($n = 3$) and *db/m* ($n = 3$) mice. Statistical analyses in **A–C** were performed using Student's *t*-test. ** $P < 0.01$; *** $P < 0.001$.

pathways that drive these illnesses is essential for crafting successful therapies. In this study, we used bioinformatics and systems biology methods to explore the common molecular processes in T2D and NAFLD.

Our study revealed 53 DEGs between T2D and NAFLD. These DEGs were associated with various biological processes, including signal transduction, transcriptional regulation, cell proliferation, gene expression, and apoptosis. To gain insight into the pathways involved, we conducted KEGG enrichment analyses. The results indicated that the ferroptosis signaling pathway was most significantly affected. Ferroptosis is a type of regulated cell death dependent on iron, characterized by the accumulation of lipid peroxides [21]. Several studies suggested that ferroptosis was involved in the dysfunction and death of pancreatic β -cells in T2D [22, 23]. This process contributes to the loss of insulin-producing cells, exacerbating glucose intolerance and diabetes progression.

To validate these predictions, we established a type 2 diabetic mouse model with NAFLD. Additionally, we measured the mRNA expression levels of *FYN*, *HNRNPU*, and *FUBP1* in the liver tissues of *db/db* and *db/m* mice. The qRT-PCR results confirmed that these

genes were differentially expressed, which is consistent with the results of the PPI analysis.

The Fyn protein [24] produced by the *FYN* gene, is involved in various biological processes such as cell proliferation, differentiation, migration, and immune responses [25, 26]. The link between the *FYN* gene and diabetes has been investigated in several studies. Under high-glucose conditions, Fyn activated and promoted the activation of Rho-associated coiled-coil containing protein kinase, leading to F-actin reorganization and subsequent podocyte damage [27]. Among mice predisposed to prediabetes due to a high-fat diet, Fyn kinase expression and activation in the spinal cord increased, resulting in heightened sensitivity to touch and diminished response to heat [28].

The association between the *FYN* gene and NAFLD has been investigated in a study [27]. Fyn kinase may influence intestinal epithelial permeability, a critical factor implicated in the development of NAFLD. When this barrier is compromised, it allows more bacterial endotoxins to enter, which can lead to liver inflammation and the onset of steatohepatitis [29].

The *HNRNPU* gene encodes a multifunctional protein that plays a vital role in RNA binding, gene transcription regulation,

chromatin organization, and the cellular response to DNA damage [30, 31]. This protein is crucial for maintaining cellular functions, and its dysregulation is associated with various diseases, including cancer and diabetes [32, 33]. *HNRNPU*, along with related heterogeneous nuclear ribonucleoproteins (hnRNPs), significantly modulates gene expression related to insulin regulation, oxidative stress, and kidney function, which are particularly relevant in the context of diabetes [34]. These proteins contribute to protective effects against common diabetes complications, such as hypertension and kidney injury, positioning them as potential therapeutic targets for managing diabetic conditions.

Even though the connection between the *HNRNPU* gene and NAFLD hasn't been extensively researched, studies on hnRNPs in liver diseases, including NAFLD, provide important insights. A research examining gene expression in liver tissues has identified differential expression of several genes, including those encoding hnRNPs, among patients with NAFLD [35]. These findings suggest a potential role for hnRNPs in the pathogenesis of NAFLD.

The *FUBP1* gene encodes Far Upstream Element-Binding Protein 1 (Fubp1) [36], which is instrumental in regulating gene expression, particularly that of the *c-Myc* oncogene [37]. This protein plays critical roles in various cellular processes, including cell proliferation, apoptosis, and differentiation [36]. Notably, *FUBP1* upregulates hexokinase genes (*HK1* and *HK2*), which are key enzymes in the glycolysis pathway. Glycolysis is essential for glucose metabolism, making its regulation directly relevant to diabetes, as disruptions in these pathways can lead to insulin resistance and glucose homeostasis issues [38].

The regulation of the *c-Myc* oncogene by *FUBP1* is important in the context of liver diseases. Dysregulation of these processes can contribute to NAFLD, by affecting liver cell turnover and survival [39]. While direct evidence linking *FUBP1* to diabetes and NAFLD is not well-established, its roles in gene regulation, metabolism, and cell survival suggest it could indirectly influence the development and progression of these conditions.

This study was preliminary and had several limitations. Further experimental studies are warranted to explore the specific roles and regulatory mechanisms of these genes and their pathways in T2D and NAFLD pathogenesis.

CONCLUSION

This study provides valuable insights into the molecular mechanisms underlying the development of T2D and NAFLD. The identified hub genes and pathways present promising prospects as therapeutic targets to address these prevalent metabolic disorders.

DATA AVAILABILITY

The data of this article will be shared on reasonable request to the corresponding author.

REFERENCES

- Elliott P, Joslin. The Prevention of Diabetes Mellitus. *JAMA* 2021;325:190.
- Lovic D, Piperidou A, Zografou I, Grassos H, Pittaras A, Manolis A. The Growing Epidemic of Diabetes Mellitus. *Curr Vasc Pharmacol*. 2020;18:104–9.
- Cole JB, Florez JC. Genetics of diabetes mellitus and diabetes complications. *Nat Rev Nephrol*. 2020;16:377–90.
- Liu Z, Zhang Y, Graham S, Wang X, Cai D, Huang M, et al. Causal relationships between NAFLD, T2D and obesity have implications for disease subphenotyping. *J Hepatol*. 2020;73:263–76.
- Younossi ZM, Koenig AB, Abdelatif D, Fazel Y, Henry L, Wymer M. Global epidemiology of nonalcoholic fatty liver disease—Meta-analytic assessment of prevalence, incidence, and outcomes. *Hepatology*. 2016;64:73–84.
- Ferguson D, Finck BN. Emerging therapeutic approaches for the treatment of NAFLD and type 2 diabetes mellitus. *Nat Rev Endocrinol*. 2021;17:484–95.
- Younossi ZM, Golabi P, de Avila L, Paik JM, Srishord M, Fukui N, et al. The global epidemiology of NAFLD and NASH in patients with type 2 diabetes: A systematic review and meta-analysis. *J Hepatol*. 2019;71:793–801.
- Lonardo A, Ballestri S, Guaraldi G, Nascimbeni F, Romagnoli D, Zona S, et al. Fatty liver is associated with an increased risk of diabetes and cardiovascular disease - Evidence from three different disease models: NAFLD, HCV and HIV. *World J Gastroenterol*. 2016;22:9674–93.
- Lu H, Zeng L, Liang B, Shu X, Xie D. High prevalence of coronary heart disease in type 2 diabetic patients with non-alcoholic fatty liver disease. *Arch Med Res*. 2009;40:571–5.
- Byrne CD, Targher G. NAFLD: a multisystem disease. *J Hepatol*. 2015;62:S47–S64.
- Powell EE, Wong VW-S, Rinella M. Non-alcoholic fatty liver disease. *Lancet*. 2021;397:2212–24.
- Kumar V, Xin X, Ma J, Tan C, Osna N, Mahato RI. Therapeutic targets, novel drugs, and delivery systems for diabetes associated NAFLD and liver fibrosis. *Adv Drug Deliv Rev*. 2021;176:113888.
- Garg K, Brackett S, Hirsch IB, Garg SK. NAFLD/NASH and Diabetes. *Diabetes Technol Ther*. 2020;22:S174–86.
- Barrett T, Wilhite SE, Ledoux P, Evangelista C, Kim IF, Tomashevsky M, et al. NCBI GEO: archive for functional genomics data sets-update. *Nucleic Acids Res*. 2013;41:D991–5.
- Dennis G, Sherman BT, Hosack DA, Yang J, Gao W, Lane HC, et al. DAVID: Database for Annotation, Visualization, and Integrated Discovery. *Genome Biol*. 2003;4:P3.
- Szklarczyk D, Gable AL, Nastou KC, Lyon D, Kirsch R, Pyysalo S, et al. The STRING database in 2021: customizable protein-protein networks, and functional characterization of user-uploaded gene/measurement sets. *Nucleic Acids Res*. 2021;49:D605–12.
- Chin C-H, Chen S-H, Wu H-H, Ho C-W, Ko M-T, Lin C-Y. cytoHubba: identifying hub objects and sub-networks from complex interactome. *BMC Syst Biol*. 2014;8:S11.
- Benjamini Y. HY: Controlling the false discovery rate: a practical and powerful approach to multiple testing. *J Royal Stat Soc Ser B*. 1995;57:289–300.
- Davis TME. Diabetes and metabolic dysfunction-associated fatty liver disease. *Metabolism*. 2021;123:154868.
- Targher G, Corey KE, Byrne CD, Roden M. The complex link between NAFLD and type 2 diabetes mellitus - mechanisms and treatments. *Nat Rev Gastroenterol Hepatol*. 2021;18:599–612.
- Jiang X, Stockwell BR, Conrad M. Ferroptosis: mechanisms, biology and role in disease. *Nat Rev Mol Cell Biol*. 2021;22:266–82.
- Sha W, Hu F, Xi Y, Chu Y, Bu S. Mechanism of Ferroptosis and Its Role in Type 2 Diabetes Mellitus. *J Diabetes Res*. 2021;2021:9999612.
- Sun Y, Bai Y-P, Wang D-G, Xing Y-J, Zhang T, Wang W, et al. Protective effects of metformin on pancreatic β -cell ferroptosis in type 2 diabetes in vivo. *Biomed Pharmacother*. 2023;168:115835.
- Nygaard HB. Targeting Fyn Kinase in Alzheimer's Disease. *Biol Psychiatry*. 2018;83:369–76.
- Peng S, Yin Y, Zhang Y, Zhu F, Yang G, Fu Y. FYN/TOPK/HSPB1 axis facilitates the proliferation and metastasis of gastric cancer. *J Exp Clin Cancer Res*. 2023;42:80.
- Peng S, Fu Y. FYN: emerging biological roles and potential therapeutic targets in cancer. *J Transl Med*. 2023;21:84.
- Lv Z, Hu M, Ren X, Fan M, Zhen J, Chen L, et al. Fyn Mediates High Glucose-Induced Actin Cytoskeleton Reorganization of Podocytes via Promoting ROCK Activation In Vitro. *J Diabetes Res*. 2016;2016:5671803.
- Suo M, Wang P, Zhang M. Role of Fyn-mediated NMDA receptor function in prediabetic neuropathy in mice. *J Neurophysiol*. 2016;116:448–55.
- Rahman K, Desai C, Iyer SS, Thorn NE, Kumar P, Liu Y et al: Loss of Junctional Adhesion Molecule A Promotes Severe Steatohepatitis in Mice on a Diet High in Saturated Fat, Fructose, and Cholesterol. *Gastroenterology* 2016;151:733–746.
- Shi Z-D, Hao L, Han X-X, Wu Z-X, Pang K, Dong Y, et al. Targeting HNRNPU to overcome cisplatin resistance in bladder cancer. *Mol Cancer*. 2022;21:37.
- Sapir T, Kshirsagar A, Gorelik A, Olender T, Porat Z, Scheffer IE, et al. Heterogeneous nuclear ribonucleoprotein U (*HNRNPU*) safeguards the developing mouse cortex. *Nat Commun*. 2022;13:4209.
- Han B-Y, Liu Z, Hu X, Ling H. HNRNPU promotes the progression of triple-negative breast cancer via RNA transcription and alternative splicing mechanisms. *Cell Death Dis*. 2022;13:940.
- Lee S, Ochoa E, Badura-Stronka M, Donnelly D, Lederer D, Lynch SA, et al. Germline pathogenic variants in *HNRNPU* are associated with alterations in blood methylome. *Eur J Hum Genet*. 2023;31:1040–7.
- Shen X, Zhang Y, Ji X, Li B, Wang Y, Huang Y, et al. Long Noncoding RNA *lncRHL* Regulates Hepatic VLDL Secretion by Modulating *hnRNPU/BMAL1/MTTP* Axis. *Diabetes*. 2022;71:1915–28.
- Bragoszewski P, Habiore A, Walewska-Zielecka B, Ostrowski J. Expression of genes encoding mitochondrial proteins can distinguish nonalcoholic steatosis from steatohepatitis. *Acta Biochim Pol*. 2007;54:341–8.

36. Ebersberger S, Hipp C, Muloz MM, Buchbender A, Hubrich D, Kang H-S et al: FUBP1 is a general splicing factor facilitating 3' splice site recognition and splicing of long introns. *Mol Cell* 2023;83:2653–2672.
37. Wang X, Xing L, Yang R, Chen H, Wang M, Jiang R, et al. The circACTN4 interacts with FUBP1 to promote tumorigenesis and progression of breast cancer by regulating the expression of proto-oncogene MYC. *Mol Cancer*. 2021;20:91.
38. Kang M, Lee SM, Kim W, Lee K-H, Kim D-Y. Fubp1 supports the lactate-Akt-mTOR axis through the upregulation of Hk1 and Hk2. *Biochem Biophys Res Commun*. 2019;512:93–99.
39. Frost JR, Mendez M, Soriano AM, Crisostomo L, Olanubi O, Radko S et al: Adenovirus 5 E1A-Mediated Suppression of p53 via FUBP1. *J Virol* 2018;92:e00439-18.

ACKNOWLEDGEMENTS

We thank all the public database used in the study, for example, GEO database, DAVID database, and STRING database. The authors wish to thank Han Wang, Jiuyu Yang, and Yutian Lei for excellent technical support.

AUTHOR CONTRIBUTIONS

Chao Chen and Zheng Wan conceived and designed the experiments; Chao Chen, Zheng Wan and Yuhan Zhang performed the experiments; Chao Chen and Zheng Wan analyzed the results; Chao Chen, Zheng Wan, Kunhuan Yang, Meiqi Lu and Xiaoyan Zhao wrote the draft. All authors have read and agreed to the published version of the manuscript.

FUNDING

This work was supported by the National Natural Science Foundation of China (Grant No. 82301227, to C.C.), the Fujian Provincial Natural Science Foundation of China (Grant No. 2023J05049, to C.C.), the Youth Innovation Grant of Xiamen (Grant No. 3502Z202371017, to C.C.), the Scientific Research Funds of Huaqiao University (Grant No. 22B5115, to C.C.), and the Fujian Provincial Natural Science Foundation of China (Grant NO. 2022J05298, to Z.W.).

COMPETING INTERESTS

The authors declare no competing interests.

ETHICS APPROVAL AND CONSENT TO PARTICIPATE

(a) The study was approved by the Huaqiao University Animal Research Ethics Committee (Approval No. A2023047). All procedures involving animals were performed in compliance with the experimental animal guidelines of Huaqiao University. (b) This study involving human subjects, human material, or human data is all from the open public database. Ethical review and approval were waived, as all the data is freely available from public dataset, for example, GEO database, DAVID database, and STRING database.

ADDITIONAL INFORMATION

Correspondence and requests for materials should be addressed to Chao Chen or Zheng Wan.

Reprints and permission information is available at <http://www.nature.com/reprints>

Publisher's note Springer Nature remains neutral with regard to jurisdictional claims in published maps and institutional affiliations.



Open Access This article is licensed under a Creative Commons Attribution-NonCommercial-NoDerivatives 4.0 International License, which permits any non-commercial use, sharing, distribution and reproduction in any medium or format, as long as you give appropriate credit to the original author(s) and the source, provide a link to the Creative Commons licence, and indicate if you modified the licensed material. You do not have permission under this licence to share adapted material derived from this article or parts of it. The images or other third party material in this article are included in the article's Creative Commons licence, unless indicated otherwise in a credit line to the material. If material is not included in the article's Creative Commons licence and your intended use is not permitted by statutory regulation or exceeds the permitted use, you will need to obtain permission directly from the copyright holder. To view a copy of this licence, visit <http://creativecommons.org/licenses/by-nc-nd/4.0/>.

© The Author(s) 2024